

3D-Printing of Zeolitic Permeable Reactive Barrier (PRB) and its Adsorptive Performance in Heavy Metal Removal

Liza Bautista-Patacsil^{a,*}, Marc Angelo Magbitang^a, Marc Jason Atega^a, Ramon Christian Eusebio^a, Myra Borines^a, Reymark Maalihan^b, Monet Concepcion Detras^a

^a Department of Engineering Science, College of Engineering and Agro-Industrial Technology, University of the Philippines Los Baños, College, Los Baños, Laguna 4031 Philippines

^b Department of Coatings and Polymeric Materials, North Dakota State University, Fargo, ND 58102 United States
 lbatacsil@up.edu.ph

Zeolite has been proven to be an effective material for heavy metal adsorption from wastewater, commonly utilized in granular form packed in fixed column beds. Other studies have suggested that compact monolithic structures in column adsorbent and catalyst applications exhibit superior adsorption kinetics and lower pressure drops, resulting in reduced maintenance requirements and enhanced performance. This study aims to investigate the feasibility of incorporating zeolite into 3D-printed monoliths for flowthrough adsorption of iron (II) from synthetic single-component acid mine drainage solutions. 3D-printed permeable reactive barrier (PRB) structures were produced through direct-ink writing using an Eazao Bio 3D ceramic printer with the following printing parameters: 1.2 mm nozzle diameter, 11 mm/s printing speed, and 0.4 MPa extrusion pressure. A 2² factorial design was employed to assess the effects of zeolite:binder ratio and printing layer on the compressive strength of the printed PRB. The optimal PRB formulation was further investigated by assessing the effects of zeolite:binder ratio and solution flow rate on the Fe removal efficiency of the PRB after column adsorption. A maximum strength of 1.24 MPa was achieved at a 0.5 mm layer height. Leaching of iron was prominent during column adsorption, resulting in only 7.25% Fe removal, possibly due to the acidity of the solution causing the displacement and release of Fe ions in the effluent. Further studies are recommended to explore ways to minimize Fe leaching and enhance the economic potential and performance of the 3D-printed PRB.

1. Introduction

Wastewater streams containing harmful pollutants are a cause for concern due to the environmental and public health risks they pose. Global economic development, continuous industrialization, and urbanization have led to an increase in both the quantity and composition of generated waste (Khajuria et al., 2009). In this study, a heavy metal of particular interest is iron (Fe). Heavy metal contamination in the Mangonbangon River in Tacloban, Philippines, showed that Fe at an average concentration of 22 g/kg was found in sediments of the river. The source for the Fe contamination was linked to weathering, erosion, as well as anthropogenic sources such as agricultural runoff, industrial wastewater discharge and mining (Decena et al., 2017). Adsorption using zeolite stands out as one of the most effective wastewater treatment methods due to its highly reactive anionic structure, making it widely used for the removal of cationic heavy metals in wastewater (Yoldi, 2019). Zeolites typically come in granular form, as is the case for most studies on zeolite adsorption. These powdered adsorbents have small particle sizes that make them challenging to separate from aqueous solutions. There is a need to devise methods to address this issue and improve the practicality and reusability of these adsorbents by eliminating tedious separation processes for the recovery of spent adsorbents (Bacelo et al., 2020). To enhance sustainability and recyclability, zeolites can be incorporated into PRBs, which have been widely used as an in situ passive treatment method for wastewater with great success. 3D monolithic structures for use as PRBs can be created through 3D printing, allowing precise control of geometry and composition. These 3D-printed structures hold significant potential as an alternative to the grains or pellets commonly employed in

typical PRBs because their open-channel structures reduce resistance to fluid flow, thereby minimizing pressure drop and increasing mass transfer (Lawson et al., 2021).

2. Materials and Methods

2.1 Preparation of Materials

A suitable 3D CAD model was initially created in AutoCAD and then converted to .gcode format for utilization in the Eazao Bio 3D Ceramic Printer. Natural zeolite (325-mesh) was acquired from LITHOS Manufacturing, with a measured Si:Al ratio of approximately 3.29. This zeolite underwent a pretreatment process, including sieving with a 125 µm mesh sieve, soaking in distilled water for 24 hours, and oven heating at 150 °C for 5 hours. It was pulverized using a mortar and pestle. Calcium bentonite, obtained from LITHOS Manufacturing, served as the binder. Reagent-grade (95% purity) hydroxyethylcellulose (HEC), acquired from Chemical.id in Indonesia, was used as a suspension aid additive. Ten (10) wt% partially-hydrolyzed polyvinyl alcohol (PVA BP-24), obtained from Dalkem Corporation in the Philippines, was used as a plasticizer. Reagent grade FeSO₄·7H₂O (97% purity) and 1 M sulfuric acid (RCI Labscan, Thailand) were used to prepare the single-component synthetic acid mine drainage solutions with about 19 ppm concentration.

2.2 Development of 3D-Printed PRB

The zeolite paste utilized for 3D printing was formulated with a 52:48 w/w ratio of powder mix to PVA solvent. The PVA solvent was prepared by dissolving 3.6 g of PVA powder into 36 mL of distilled water. The powder mix, consisting of zeolite, bentonite, and HEC, was manually mixed in a separate container before combining it with the PVA solution. Table 1 presents the weighed amounts of the ink paste components at different zeolite:binder ratios, which were employed for each batch of two PRBs.

Table 1: Weight composition of the 3D printable zeolite paste.

Zeolite:binder ratio, %w/w	Zeolite, g	Bentonite, g	HEC, g	PVA solution, mL
80:20	30.420	7.605	0.975	36
85:15	32.321	5.704	0.975	36
90:10	34.223	3.803	0.975	36

Using the Eazao Bio 3D Ceramic Printer, the mixture of powder-PVA solution was loaded into the cartridge, and printing parameters were set. A nozzle diameter of 1.2 mm, printing speed of 11 mm/s, and layer heights of 0.5 mm, 0.6 mm, and 0.7 mm were utilized, with an air extrusion pressure of 0.4 MPa. After printing, the PRBs were air-dried for 4 days in a closed cabinet. After drying, calcination post-treatment was performed by subjecting the dried PRBs to furnace heating at 550 °C for 1 hour under inert conditions.

2.3 Characterization of PRB

Thermogravimetric analysis (TGA) was performed at NASAT Labs using the Hitachi NEXTA STA 200 RV to evaluate the thermal stability of the PRBs, employing a ramping temperature mode from 0 °C to 1000 °C. Fourier Transform Infrared Spectroscopy (FTIR) was conducted at OneLab DOST-FPRDI using the Shimadzu IR Prestige 21 Fourier Transform Infrared Spectrophotometer, equipped with Single Reflection Diamond Attenuated Total Reflectance (ATR), to ascertain the composition of the PRBs before and after calcination. Lastly, scanning electron microscopy and energy dispersive X-ray spectroscopy (SEM-EDX) were conducted at NASAT Labs using the Hitachi TM4000 Plus and Oxford Xplore Compact 30, respectively, to analyze the surface appearance and characteristics of the PRB, as well as the relative elemental compositions.

2.4 Mechanical Strength Test

A compressive strength test was conducted to determine the optimal formulation conditions for the 3D-printed PRB. The ASTM D695 standard compressive strength test was carried out at OneLab DOST-FPRDI to measure compressive strength at varying zeolite:binder ratios (80:20, 85:15, 90:10 w/w) and layer heights (0.5, 0.6, 0.7 mm). A 2² full factorial design was performed with two (2) replicates and three (3) center points using uncalcined PRBs. Design-Expert® version 13 was employed to identify the best formulation conditions.

2.5 Column Adsorption Test

PRBs printed with the optimal formulation conditions underwent column adsorption at varying zeolite:binder ratios (80:20, 85:15, 90:10 w/w) and solution flow rates (1, 2, 3 ml/min) to assess removal efficiency. The initial and final residual heavy metal concentrations were measured using Shimadzu AA-7000 to determine the

removal efficiency of the 3D-printed adsorbent. Design-Expert® version 13 was also utilized to determine the optimal conditions for removal efficiency.

3. Results and Discussion

3.1 Development of 3D Printed PRB

The prototypes of 3D-printed zeolitic PRB were successfully developed. The uncalcined and calcined PRB are shown in Figure 1. A powder mix to PVA solvent ratio of 52:48 % w/w provided the best consistency for the formulation of 3D PRB.

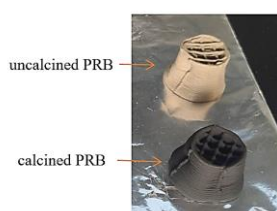


Figure 1: Visual comparison of the uncalcined and calcined 3D-printed PRB.

3.2 PRB Characterization

The infrared (IR) spectra (% Absorbance vs. Wavelength), as depicted in Figure 2, illustrate the removal of functional groups linked to polyvinyl alcohol before and after the calcination of the PRB. There is a significant reduction in the OH functional groups from approximately 0.17% to 0.08% absorbance, indicating the successful removal of the PVA content from the PRB after calcination. This reduction could potentially diminish the likelihood of blocking ion exchange sites in the zeolite, hindering effective adsorption (Kharazmi et al., 2015). A shift in the peak position associated with SiO_4 and AlO_4 stretching suggests the occurrence of dealumination after the calcination process (Olegario et al., 2017).

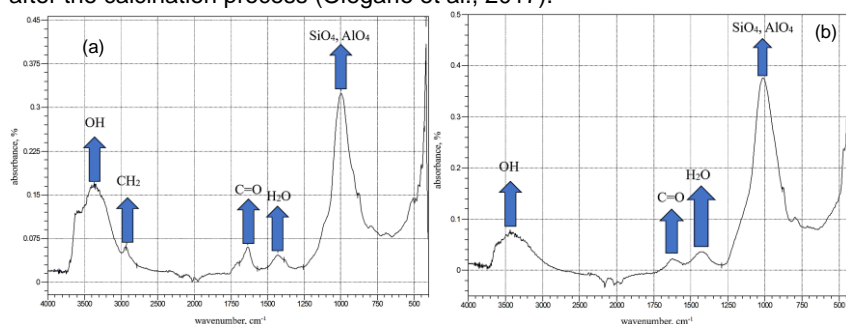


Figure 2: FTIR spectra of (a) uncalcined and (b) calcined PRB.

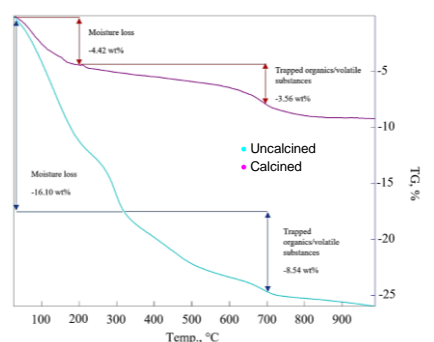


Figure 3: TGA plots of uncalcined and calcined PRB.

Figure 3 presents the thermogravimetric analysis (TGA) plots of both uncalcined and calcined PRBs, revealing distinct thermal behaviours in terms of corresponding weight losses. The uncalcined sample exhibited a significant moisture loss of 16.10 wt% up to $\sim 200^\circ\text{C}$, indicative of high physically adsorbed water content, and a further weight loss of 8.54 wt% up to $\sim 700^\circ\text{C}$ due to the decomposition of trapped organics and volatile substances from PVA and HEC (Gili & Olegario, 2021). In contrast, the calcined sample showed a much lower

moisture loss of 4.42 wt% and a reduced weight loss of 3.56 wt% for the same respective temperature ranges, highlighting the effectiveness of calcination in removing these components. This process significantly enhances the thermal stability of the calcined sample, making it more suitable for high-temperature applications by reducing moisture and organic content (Khalil et al., 2021).

3.3 Mechanical Strength Test Results

The selected factors for assessing their effects on the mechanical strength of the PRB were zeolite:binder ratio (80:20, 85:15, and 90:10 w/w) and printing layer height (0.5, 0.6, 0.7 mm). ANOVA results indicate a significant model, with zeolite:binder ratio showing no significant effect on strength, while printing layer height demonstrates an inverse relationship with mechanical strength as shown in Figure 4. This is consistent with the findings of Druga et al. (2021), where decreasing the layer height increased the contact area between layers, resulting in higher mechanical strength. Uncalcined zeolitic PRB exhibited an average compressive strength of 6.4224 MPa, while calcined PRB averaged 1.1822 MPa. These results are higher than that obtained by Thakkar et al. (2016), which measured an average of 0.69 MPa in their 3D-printed zeolite monolith.

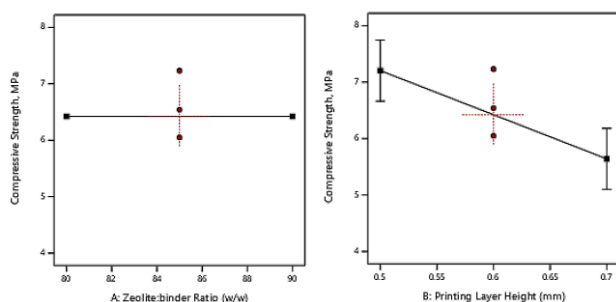


Figure 4: Effect of zeolite:binder ratio and printing layer height on compressive strength.

3.4 Column Adsorption Test Results

The residual Fe concentration was measured at varying zeolite:binder ratios (80:20, 85:15, and 90:10 w/w) and solution flow rates (1, 2, 3 mL/min). Figure 5 presents the contour map and 3D surface response map of the column adsorption tests using calcined PRBs. ANOVA results at 95% confidence interval indicate a significant model where zeolite:binder ratio (p -value = 0.0242) and solution flow rate (p -value < 0.0001) were both significant factors.

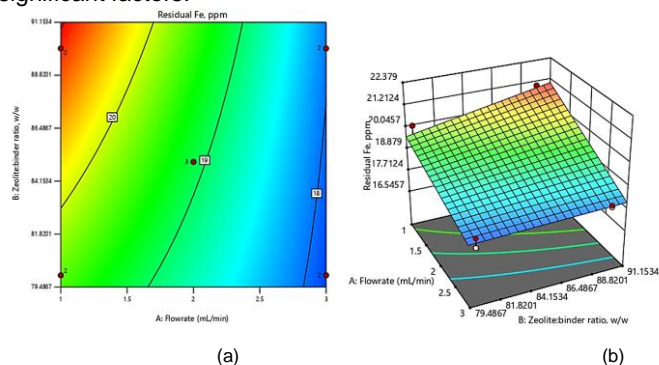


Figure 5: Residual Fe (a) contour map and (b) 3D surface response map of the 3D printed PRB.

A minimum residual Fe concentration of 17.622 ppm, corresponding to a 7.25% removal efficiency, was observed at an 80:20 w/w zeolite: binder ratio and a 3 mL/min solution flow rate. The residual Fe concentration increased with a higher zeolite:binder ratio, contrary to Thakkar et al.'s (2016) findings. This could be due to the leaching of Fe content within the zeolite into the treated effluent, possibly caused by the low pH of the influent displacing Fe ions from the zeolite. The calcination step was intended to stabilize the Fe present in the PRB by oxidizing them into more stable iron oxides such as Fe_2O_3 , which are less prone to leaching under acidic conditions. However, Fe leaching was still observed during column adsorption experiments, particularly at treatments with lower flowrates (higher contact time between the acidic solution and zeolite), and higher zeolite:binder ratios (higher leachable Fe content in the PRB). Based on these observations, further studies are recommended to reduce the Fe present in the zeolite through methods such as mild acid washing or determining the optimum pH for PRB utilization to mitigate iron leaching and enhance the overall effectiveness of the PRB

in heavy metal removal. The 3D-printed PRBs are designed not only for Fe removal but also for other heavy metals present in acid mine drainage (AMD) effluents such as copper. Results showed that the combination of 90 wt% adsorbent loading and a 1 mL/min flowrate are the optimal values for achieving the maximum removal efficiency of copper (II) using the 3D printed PRB. The maximum values obtained are 15.328% and 49.099% for uncalcined and calcined PRB, respectively. To achieve complete removal of copper (II), a series of sorption experiments can be conducted.

3.5 Results of SEM-EDX Characterization

In Figure 6, a comparison of SEM images for uncalcined, calcined, and Fe-sorbed PRBs at 25x and 1000x magnifications are presented. The uncalcined PRB appears to have fewer visible pores and a smoother surface, while the calcined and Fe-sorbed PRBs exhibit more visible pores. The surface of the uncalcined PRB may also show smooth chunks, likely PVA particles. In contrast, the surfaces of the calcined and Fe-sorbed PRBs display distinct particles, visible pores, and a crystalline appearance. The Fe-sorbed PRB retains a crystalline surface even after adsorption tests, and Fe adsorbate particles may be present.

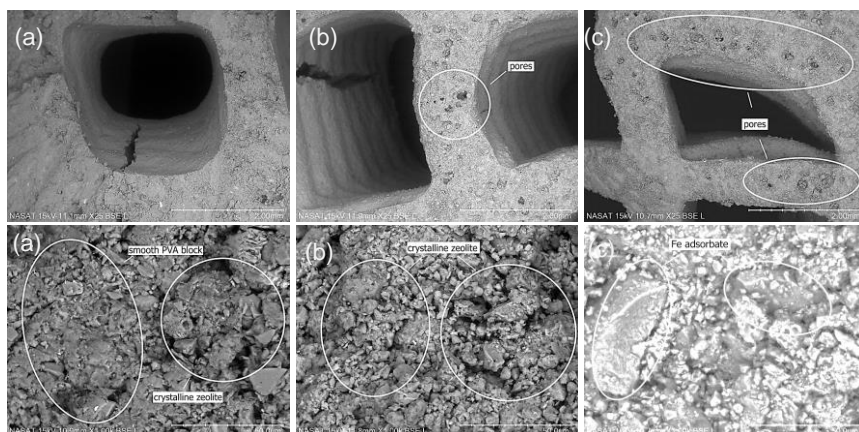


Figure 6. SEM images showcasing the microstructure of the samples: (a) uncalcined, (b) calcined, and (c) Fe-sorbed PRBs, each at their respective magnifications.

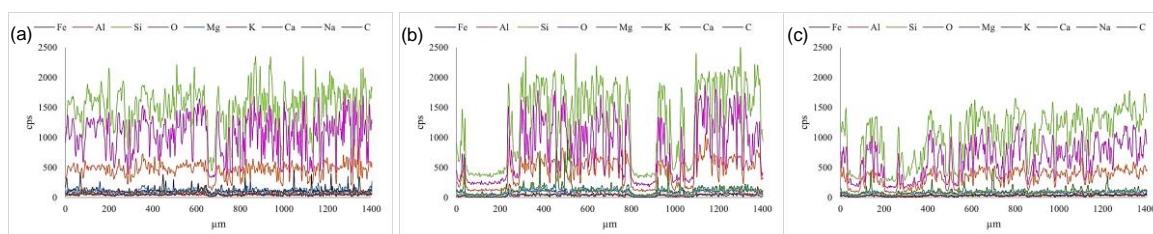


Figure 7: EDX analyses of (a) uncalcined, (b) calcined, (c) Fe-sorbed PRBs.

EDX line analysis was conducted to examine the relative elemental composition of the PRBs. Figure 7 illustrates the EDX line graphs for uncalcined, calcined, and Fe-sorbed PRBs. The samples predominantly contain Si as the most abundant element, followed by Al and O. Additionally, relatively low intensities of other elements such as Fe, Ca, K, Na, and Mg can be observed, which are typically present in lower amounts in zeolite and bentonite. Moreover, the calcined sample appears to have multiple gaps in the spectra, indicating the presence of porous areas where little or no elements were detected. In the Fe-sorbed sample, less gaps are visible compared to the calcined spectra, which could indicate adsorption in the PRB thereby reducing the number of porous spaces. EDX analysis also shows an average decrease in the Fe intensity of the sorbed PRB by 16% compared to the calcined PRB, which further indicates occurrence of leaching. This could also explain the relative decrease in Si and O intensity. A study by Saifuddin et al. (2019) suggests that Fe adsorbate particles may have formed ligand complexes with the surface functional groups of the zeolite, which could have also leached from the PRB during treatment.

4. Conclusions

The successful development of a 3D-printed zeolitic permeable reactive barrier (PRB) is a noteworthy achievement. This study demonstrated sufficient mechanical strength, aligning with findings from other column

adsorption studies and proving suitable for lab-scale adsorption experiments. Analyses through TGA, FTIR, and SEM-EDX confirmed the successful removal of PVA from the PRB after calcination. The structure's rigidity was maintained post-calcination, contributing to improved porosity that endured even after adsorption tests. The highest removal efficiency achieved with the calcined PRB was 7.25%, notably lower than that of typical granular adsorbents. This discrepancy may stem from the reduction in surface area when transitioning from granular to 3D-printed zeolite. Leaching of Fe ions from the adsorbent into the treated effluent may have occurred. SEM-EDX line analysis revealed a decrease in Fe intensity after column adsorption, suggesting the release of Fe from the PRB into the influent. Previous studies propose that this phenomenon is accentuated in a low pH environment. The solution's acidity at pH 3 may have led to the displacement of Fe ions within the zeolite framework by the high concentration of H⁺ ions, releasing Fe ions into the solution. The range of Fe concentration of 17.622 ppm to more than 21 ppm found may not indicate the desired characteristic for Fe adsorption, but it is an indicator of the presence of leaching during adsorption. Hence, it is imperative to address leaching issues and enhance the PRB's performance. Leaching of Fe in related methodologies was present but minimal; therefore, future studies may be structured more similarly to restrict the conditions suitable for Fe, i.e., less acidic pH, and increase pretreatment procedures to "lock" in the surface Fe ions. A higher removal of 49.099%, on the contrary, was obtained for the adsorption of Cu (II). Performing the sorption experiments in series is recommended to achieve complete removal of Cu (II) from single AMD solution. Further improvements are essential to mitigate leaching and bring the PRB into compliance with water quality guidelines.

Acknowledgments

This work was funded by the UP System Enhanced Creative Work and Research Grant (ECWRG-2022-1-10R).

References

- Bacelo, H., Pintor, A. M., Santos, S. C., Boaventura, R. A., & Botelho, C. M. (2020). Performance and prospects of different adsorbents for phosphorus uptake and recovery from water. *Chemical Engineering Journal*, 381, 122566.
- Druga, C., Şerban, I., Braun, B., & Tulica, A. (2021). Analysis of the Influence of the Layer Height on the Strength of 3d Printed Structures.
- Khalil, A., Hashaikh, R., & Hilal, N. (2021). 3D printed zeolite-Y for removing heavy metals from water. *Journal of Water Process Engineering*, 42, 102187.
- Khajuria, A., Yamamoto, Y., & Morioka, T. (2010). Estimation of municipal solid waste generation and landfill area in Asian developing countries. *Journal of environmental biology*, 31(5), 649-654.
- Kharazmi, A., Saion, E., Faraji, N., & Mahmoon Yat Yunus, W. (2015). Structural, optical, opto-thermal and thermal properties of ZnS-PVA nanofluids synthesized through a radiolytic approach. *Beilstein J. Nanotechnology*, 6, 529-536.
- Lawson, S., Li, X., Thakkar, H., Rownaghi, A. A., & Rezaei, F. (2021). Recent advances in 3D printing of structured materials for adsorption and catalysis applications. *Chemical Reviews*, 121(10), 6246-6291.
- Olegario-Sanchez, E., Felizco, J. C., & Mulimbayan, F. (2017, December). Investigation of the thermal behavior of Philippine natural zeolites. In *AIP Conference Proceedings* (Vol. 1901, No. 1). AIP Publishing.
- Olegario, E. M., & Gili, B. Z. (2021). Characterization of Philippine natural bentonite. Cambridge University Press. <https://doi.org/10.1017/exp.2021.16>
- Pacle Decena, S. C., Sanita Arguelles, M., & Liporada Robel, L. (2018). Assessing Heavy Metal Contamination in Surface Sediments in an Urban River in the Philippines. *Polish Journal of Environmental Studies*, 27(5).
- Saifuddin, M., Bae, J., & Kim, K. S. (2019). Role of Fe, Na and Al in Fe-Zeolite-A for adsorption and desorption of phosphate from aqueous solution. *Water research*, 158, 246-256.
- Thakkar, H., Eastman, S., Hajari, A., Rownaghi, A. A., Knox, J. C., & Rezaei, F. (2016). 3D-printed zeolite monoliths for CO₂ removal from enclosed environments. *ACS applied materials & interfaces*, 8(41), 27753-27761.
- Yoldi, M., Fuentes-Ordoñez, E. G., Korili, S. A., & Gil, A. (2019). Zeolite synthesis from industrial wastes. *Microporous and Mesoporous materials*, 287, 183-191.